

High Temperature Oxidation, Range of Non-Stoichiometry and Curie Point Variation of Cation Deficient Titanomagnetite $\text{Fe}_{2.4}\text{Ti}_{0.6}\text{O}_{4+\gamma}$

Z. Hauptman

(Received 1974 February 5)*

Summary

Synthetic spinel titanomagnetite of composition $\text{Fe}_{2.4}\text{Ti}_{0.6}\text{O}_{4+\gamma}$ was equilibrated with CO–CO₂ mixtures at 1275° to produce a series of samples with varying oxidation parameter γ within the monophasic stability field. After equilibrium had been attained all samples were sharply quenched in the same way. Curie temperature (T_c) was measured and the parameter γ was determined from weight changes to an accuracy of 0.01 per cent by means of Cahn Gram Electrobalance.

A very strong practically linear dependence of T_c upon oxidation parameter has been found: $T_c(\gamma) = T_c(\gamma_0) + 890\gamma$; ($0 < \gamma < 0.06$). The slope, 890 ($\text{K}\gamma^{-1}$) appears to be considerably steeper, namely by a factor of 9, than the $T_c(\gamma)$ dependence for a titanomagnetite of the same composition oxidized to its maghemite correlate, i.e. below about 350 °C. The relatively high sensitivity, reversibility and reproducibility with which the above relation is obeyed is good enough to utilize T_c as a diagnostic parameter for the degree of non-stoichiometric imbalance in titanomagnetites which were rapidly cooled, provided the iron–titanium ratio is known. This finding may explain the large scatter of values of T_c so far published (up to 60 K for $\text{Fe}_{2.4}\text{Ti}_{0.6}\text{O}_4$).

1. Introduction

Igneous rocks have been used to obtain detailed information about the ancient geomagnetic field and provide much of the experimental data on which the hypothesis of the geomagnetic dynamo, continental drift and polar wandering are based. The magnetic record stored in the majority of the igneous rocks used in palaeomagnetic studies is carried by titanomagnetites. These generally deviate from ideal composition and structure in a number of ways, e.g. in containing cations other than Fe and Ti, being non-stoichiometric to some degree, in phase inhomogeneity (exsolution and/or unmixing). The acquisition and retention of the magnetic record by these minerals depends on intrinsic physical parameters (e.g. magnetic anisotropy, Curie point) and grain volume. These parameters in turn depend on the physicochemical state of the minerals described above.

The general consistency of palaeomagnetic data in space and time indicates that the information carried by titanomagnetites is generally a faithful recording of the ancient geomagnetic field. As the nature of the process of acquisition of this record

* Received in original form 1973 October 19.

by titanomagnetites of the types occurring in rocks is increasingly worked out, so the palaeomagnetism of igneous rocks is put on a progressively sounder physical basis. The effect of cation 'impurities' (Al and Mg) on intrinsic properties of titanomagnetites has recently been studied (Richards *et al.* 1973) and the effect of low temperature ($\sim 350^\circ\text{C}$) non-stoichiometry has been the subject of extensive investigation (Ozima & Sakamoto 1972; Readman & O'Reilly, 1970, 1971, 1972). The purpose of the present work is to study non-stoichiometry produced at high temperatures ($\sim 1300^\circ\text{C}$) on an intrinsic physical parameter (Curie point).

The study of the relationship between Curie temperature and composition in metastable quenched samples of synthetic spinel titanomagnetites is of particular importance to the properties of oceanic basalts and rapidly quenched lavas. At the same time it is relevant to some aspects of ferrimagnetism in general and also to phase equilibria and the chemistry of defects in complex magnetic oxides.

Titanomagnetite, in accordance with the present nomenclature, is the common name for any member of the solid solution series between ferrous orthotitanate (mineral ulvöspinel) and magnetite: $x\text{Fe}_2\text{TiO}_4(1-x)\text{Fe}_3\text{O}_4$, where x stands for molar fraction of ulvöspinel.

We have selected for our experiments the composition $x = 0.6$ (further denoted TM60) as it represents the statistically most abundant titanomagnetite in a large collection of samples of basaltic rocks from a variety of places which have been studied at Newcastle (Creer & Ibbetson 1970).

1.1 Oxidation of titanomagnetites

Natural titanomagnetites frequently undergo oxidation to an extent which is

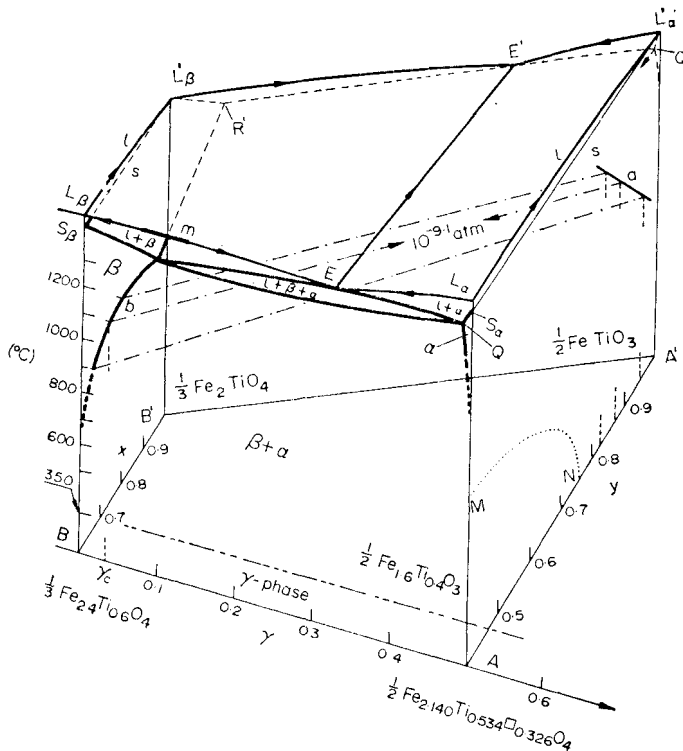


FIG. 1. Vertical pseudobinary section (plane $BL_\beta L_\alpha A$) along the oxidation line (BA) through a part of the space diagram 'FeO- Fe_2O_3 - TiO_2 '.

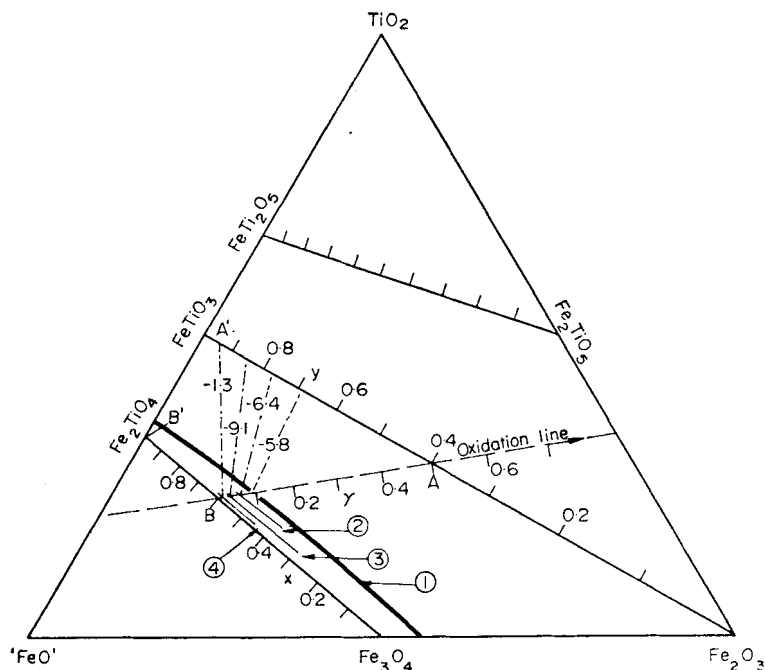
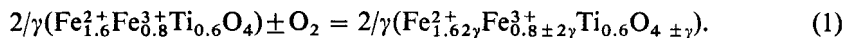


FIG. 2. A projection of the 'FeO'- Fe_2O_3 - TiO_2 ternary showing the positions of the oxidation line and of the univariant β - α boundaries with their corresponding tie lines between the β - α conjugate surfaces at several temperatures: 1-1300, $\gamma_c \approx 0.08$, 2-1275, $\gamma_c = 0.063$, 3-1100, $\gamma_c = 0.035$ and 4-900 °C, $\gamma_c \approx 0.010$.

dependent on the petrologic history of their direct environment. Oxidation of titanomagnetites poses a major problem, notably in conjunction with research into the stability of direction and intensity (J_n) of the nrm which is of fundamental importance to palaeomagnetic studies.

Addition or removal of a small amount of oxygen to or from TM60, originally stoichiometric, can be represented in the following way



When talking about oxidation of titanomagnetites one has to make a clear distinction between the low temperature (lt) oxidation, i.e. below about 350 °C which under favourable conditions leads to titanomaghemites (γ -phases, structural analogues of maghemite, $\gamma\text{-Fe}_2\text{O}_3$), and the high temperature (ht) oxidation. It is the latter which is the subject of this study. The essential difference between the lt and ht oxidation is in the extent of non-stoichiometry which the spinel phase can bear. For instance, TM60 can be oxidized in the lt region up to the maximum possible value of $\gamma_c = 0.8$ whereas ht oxidation of the same titanomagnetite at 1300 °C is restricted to $\gamma_c \approx 0.08$, (cf. Figs 1 and 2). Further oxidation beyond the critical, high temperature oxidation parameter γ_c leads to break down of the spinel phase (β) and to the nucleation and subsequent growth of the rhombohedral, haemoilmenite phase (α). As can be seen from the diagram in Fig. 1 the $\gamma_c(T)$ curve approaches zero at about 600 °C. Thus in order to study the changes in magnetic properties of a non-stoichiometric single phase titanomagnetite produced by high temperature oxidation we had to use a quenching technique sufficiently effective to preserve the monophasic spinel.

1.2 Magnetic properties of non-stoichiometric titanomagnetites

Because of their widespread occurrence in the Earth's crust titanomagnetites, oxidized in the low temperature region have been intensively studied in conjunction with rock magnetism. In contrast little is known about the relation between magnetic properties and the degree of high temperature oxidation.

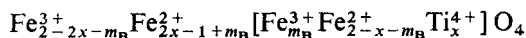
The low temperature oxidation process has certain common features with the high temperature process, e.g. the same value of γ implies the same bulk $\text{Fe}^{2+}/\text{Fe}^{3+}$ ratio and both oxidation products form cation deficient spinel lattices. It is therefore convenient in view of further considerations to survey briefly relevant results on magnetic properties, especially on Curie temperature of the titanomagnetites oxidized in the low temperature region.

Comprehensive studies of the entire low temperature oxidation range of titanomagnetites with values $x = 0.0; 0.4; 0.7$ and 1.0 have been published by Readman & O'Reilly (1970, 1971, 1972). Among other things they measured the dependence of Curie point, T_c on oxidation parameter z . (The $z-\gamma$ conversion formula: $z = 2\gamma/(1+x)$). Somewhat similar measurements were carried out by Ozima & Sakamoto (1972) with compositions $x = 0.7; 0.9$ and 1.0 .

A theoretical expression for computing Curie temperatures of both stoichiometric and oxidized titanomagnetites has been derived recently by Stephenson (1972a). He extended the Weiss molecular field theory, as applied by Néel to ferrites to more complex spinels containing two types of cations carrying magnetic moment, such as $\text{Fe}^{2+} - \text{Fe}^{3+}$ or $\text{Fe}^{3+} - \text{Ni}^{2+}$ etc. Beside the spontaneous magnetization *vs* temperature curves he has obtained a general expression for Curie temperatures. For spinels containing only Fe^{2+} and Fe^{3+} as magnetic ion (which is the case of titanomagnetites) the formula acquires a simpler form

$$T_c = 700 \left(\frac{8.4}{a} \right)^{13} \sqrt{(D - \Delta/D)}. \quad (2)$$

Here a is the lattice parameter and the terms D and Δ represent two different functions of the $\text{Fe}^{2+} - \text{Fe}^{3+}$ distribution between the tetrahedral (A) and octahedral (B) sites of the spinel lattice. The distribution for an arbitrary x value of a stoichiometric titanomagnetite can be written as follows



Square brackets contain those cations located in B sites. Thus for a stoichiometric titanomagnetite the single variable m_B , i.e. the concentration of Fe^{3+} in the B sites is sufficient to characterize the distribution (on the assumption that Ti^{4+} only occurs on octahedral sites).

It has been postulated by Stephenson (1969) that the distribution of $\text{Fe}^{2+} - \text{Fe}^{3+}$ into A and B lattice sites is temperature dependent and is governed at equilibrium by the Boltzmann relation $y(1+y)/(1-y)^2 = \exp(-\Delta E/kT)$. Here y and $1-y$ are the fraction of bivalent cations on octahedral and tetrahedral sites. The sought function $m_B(\text{equil.}) = f(T)$ for a given titanomagnetite has been derived from the latter relation and it has been shown that its extrema for $T \rightarrow 0$ and for $T \rightarrow \infty$ coincide with two models of distribution suggested earlier by Néel & Chevalier and by Akimoto. The former model represents fully ordered distribution (for which $m_B = 1-2x$, if $x \leq 0.5$ and $m_B = 0$ if $x > 0.5$) whereas the latter model represents fully disordered distribution (for which $m_B = 1-x$ applies). For instance, for the studied composition TM60 the computed values of Curie temperature in accordance with the above models are 178 and 150°C respectively. Thus highly quenched samples should exhibit a lower T_c than samples cooled slowly or annealed at lower temperatures. (Provided the activation energy barrier for the distribution process is high enough to enable efficient quenching.)

Extending the molecular field approximation to the oxidized, cation deficient titanomagnetites Stephenson (1972b) calculated the $T_c(\gamma)$ dependence for the entire compositional range ($0 \leq x \leq 1$) and the entire oxidation range ($0 \leq \gamma \leq \frac{1}{2}(1+x)$). The calculated $T_c(\gamma)$ curve for titanomagnetite TM60 is nearly linear and could be represented by the formula

$$T_c(\gamma) = T_c(\gamma_0) + \bar{k}\gamma. \quad (3)$$

The average gradient \bar{k} has two extreme values depending whether the oxidized titanomagnetite was originally ordered (N-C model) or disordered (A model). The two respective calculated values of \bar{k} for TM60 are 350 and 375 $\text{K}\gamma^{-1}$.

1.3 High temperature oxidation of titanomagnetites and the phase relationship.

The general structures of the 'FeO'- Fe_2O_3 - TiO_2 ternary space diagram in the the X-T- p_{O_2} co-ordinates has been fairly well established because of the importance of the system to earth sciences and partly also to the metallurgy of iron. However, accurate knowledge of the diagram based on direct experimental work is still rather fragmentary, and therefore in regions of particular interest it is often necessary to carry out suitable measurements to supplement incomplete and/or inaccurate data. Compiling available data and applying general rules for phase equilibria we have drawn a space diagram represented in Fig. 1. It shows the pseudobinary vertical section (the plane $\text{BL}_\beta\text{L}_\alpha\text{A}$) relevant to this study. The section is made along the oxidation line BA (i.e. the line of constant Fe/Ti ratio) which passes through the composition of TM60 (point B). The important high temperature oxidation region is the monophasic field β . We have been especially interested in fixing the exact position of the univariant phase boundary b between the β and α -phases. The phase equilibria data for the latter region were obtained from the following sources:

(i) *The critical oxidation parameter, γ_c (points on the boundary b).* $\gamma_c(1300^\circ\text{C}) \approx 0.08$, Taylor (1964); $\gamma_c(1275^\circ\text{C}) \approx 0.06$ present work; $\gamma_c(1100^\circ\text{C}) = 0.035 \pm 0.002$, present work; $\gamma_c(900^\circ\text{C}) \approx 0.01$, extrapolated from the previous points.

(ii) *The tie-lines.* (cf. also Fig. 2). 1300°C , interpolated, Taylor (1964); 1275°C estimated from present results; 1200 , 1100 and 900°C , Buddington & Lindsley (1964). The tie line at 1100°C has been confirmed in this work by the emf measurements with solid state electrolyte (see below).

(iii) *The melting equilibria.* The melting point of TM60 (point L_β in Fig. 1): 1468 ± 10 , interpolated from graphical representation of the liquidus surfaces in the 'FeO'- Fe_2O_3 - TiO_2 system, Taylor (1963); $1460 \pm 5^\circ\text{C}$, determined by thermal analysis in controlled p_{O_2} , Hauptman (1973, unpublished); maximum melting point of the partly oxidized melt (within the section m on the line L_βE): $1475 \pm 5^\circ\text{C}$, Hauptman (1973).

2. Experimental

2.1 Sample preparation and characterization

2.1.1 *Sintering procedure.* Thoroughly mixed powdered Fe(99.9 per cent, Koch & Light), Fe_2O_3 (99.8 per cent, Mapico Products) and TiO_2 (99.5 per cent, Koch & Light) in the appropriate proportions were pressed into tablets under pressure of 3 tons/cm^2 ($3 \times 10^8 \text{ Nm}^{-2}$). The tablets were placed in a recrystallized alumina boat and fired at 1325°C in an impervious sealed mullite tube filled with a buffering mixture of 90 vol. per cent argon, 6.7 vol. per cent CO_2 and 3.3 vol. per cent CO. The tablets were then crushed and milled under specially dried methanol in a tungsten carbide centrifugal ball mill down to an average particle size of $1 \mu\text{m}$. The powder was again pressed into tablets and fired under the same conditions as before.

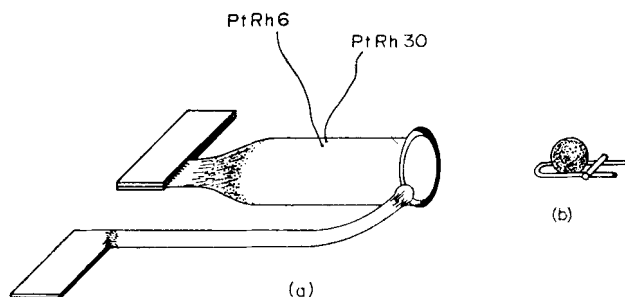


FIG. 3. Tubular platinum furnace (a) for direct resistance heating ($\sim 3V$, ~ 100 Amp, ac) with welded-on thermocouple and an iridium cradle, (b) with a spherical sample.

Metallographic tests of the final tablets revealed a low porosity (5–10 per cent), grains about $50\ \mu\text{m}$ without any stray phases. The actual samples were cut out of the central parts of the tablets and shaped into spheres of about 2-mm diameter, weighing about 25 mg. The samples prepared from the batches denoted from A to C used in some of the preliminary experiments were synthesized in a very similar manner as described above (for batches D and E) except for the temperature of firing which was 1200°C .

2.1.2 Equilibration. A specially devised little tubular furnace was used to bring the samples to equilibrium with the p_{O_2} -controlled atmospheres (Fig. 3(a)). It consists of a platinum tube of 4-mm internal diameter, 0.1 mm wall thickness, 20 mm length, with one flattened closed end. The tube is heated directly by passing ac current at low voltage through it. Because of the very low heat capacity of the furnace and a fast dissipation of the heat mainly into the water-cooled massive copper clamps the 'quenching' effect can be achieved by simply switching the current off. This method of quenching was found to be fast enough to stop abruptly any significant oxygen transfer between the gaseous buffer and the solid sample. Its other important feature was an almost exactly repeatable cooling course for all runs. The time constant, τ of the furnace is 20 s, the initial cooling rate from 1275°C is approximately $70\ \text{K s}^{-1}$. The whole furnace assembly is enclosed in a Pyrex mantle which is continuously flushed with a CO_2 -CO buffer. The spherical specimen of the titanomagnetite is supported on an iridium cradle during the heat treatment (Fig. 3(b)). Iridium was found superior to platinum when in contact with titanomagnetites in reducing atmospheres as iron from the latter diffuses into iridium at a considerably lower rate than into platinum. Typical times needed for a complete equilibration were about 1 hr.

2.1.3 Determination of the apparent oxidation parameter. The apparent oxidation parameter γ' pertinent to an adjusted value of p_{O_2} was determined after each equilibration and subsequent quenching. The change in mass of the TM60 sphere, $\pm \Delta M$ was measured against a reference weight M_r and the apparent oxidation parameter was calculated from the relation $\gamma'(\text{TM60}) = [\pm \Delta M / (M_r \pm \Delta M)] \times 14.174$. As the reference value, M_r we chose the weight at which a sample steadied when heated at 1275°C in an atmosphere of oxygen partial pressure $p_{\text{O}_2} = 10^{-7.42}$ atm. To this weight we attached the value of $\gamma' = 0$. The samples were weighed on the Cahn Gram Electrobalance with the relative accuracy of 0.01 per cent. In the value of γ' this represents an error, $\delta\gamma' = 0.002$. In the preliminary experiments (carried out with the samples TM60, batches A, B and C) we tested among other things the constancy of weight on repeated heat treatments at the same temperature and oxygen partial pressure. We found that for the range of $p_{\text{O}_2} \geq 10^{-7.5}$ (atm) the weight stayed constant within the error involved in weighing. However, on the side towards the

Table 1

Apparent oxidation parameter γ' and Curie temperatures, T_c of titanomagnetite TM60 equilibrated at various oxygen partial pressures at 1275 °C

Run No.*	Net total weight change (mg)	Apparent oxidation parameter	$\text{CO}_2/\text{CO}^\dagger$ volume ratio	$-\log p_{\text{O}_2}$	Curie temperature (°C)
Set No. 1: Sample TM60'D', reference weight 28.484 mg					
1	0.000	0.000	20	7.42	160.5
2	0.016	0.008	30	7.07	168.2
3	0.034	0.017	40	6.82	176.0
4	0.065	0.032 ₅	55	6.55	190.0
5	0.094	0.046 ₅	61	6.46	204.2
6	0.041	0.020 ₅	47	6.68	180.0
7	-0.007	-0.003 ₅	15	7.67	158.0
8	-0.013	-0.006 ₅	10	8.03	155.2
Set No. 2: Sample TM60'E', reference weight 25.814 mg					
9	0.000	0.000	20	7.42	161.5
10	0.004	0.002	26	7.30	164.5
11	0.018	0.010	36	6.92	171.0
12	0.049	0.027	52	6.60	186.0
13	0.103	0.056 ₅	61	6.46	220.0
14	0.121	0.065 ₅	65	6.41	232.5
15	-0.004	-0.002	16	7.54	159.5
16	-0.015	-0.008	9	8.12	155.0

* o, equilibrium attained by oxidation; r, equilibrium attained by reduction of the sample.

† $p_{\text{CO}_2} + p_{\text{CO}} \approx 1$ atm.

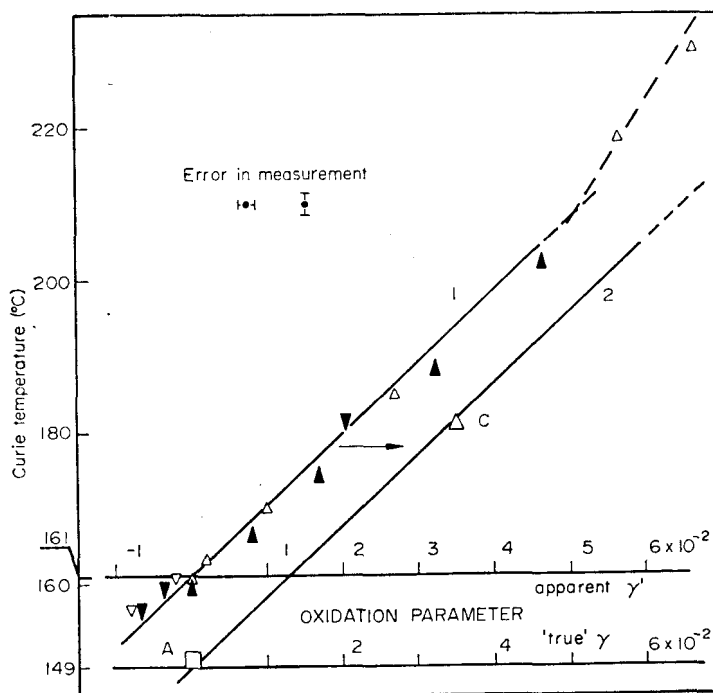


FIG. 4. The Curie temperature of TM60 as a function of the oxidation parameter γ' . The actual experimental points are the sharp vertices of the triangles whose position indicates the way in which the oxidation/reduction equilibrium value of γ was attained. Triangles pointing upwards means oxidation. Solid and open triangles correspond to samples D and E respectively. The transformation from the γ' to γ abscissae is indicated by the arrow.

lower values of p_{O_2} we have observed an increasing tendency to irreversible weight losses, most likely due to some iron diffusing into the iridium support. From this reason the pressure of about 10^{-8} (atm) O_2 presented a practical limitation to the described experimental procedure of equilibration. In the final measurements (with the samples denoted D and E) we have therefore scheduled the measurements so as to investigate the region $p_{\text{O}_2} > 10^{-7.5}$ (atm) first before exposing the samples to lower oxygen fugacities. The succession of equilibrations together with the values of the apparent oxidation parameter γ' and their corresponding Curie temperatures are given in the Table 1. The $T_c(\gamma')$ plot is shown in Fig. 4. The attempts to determine the true values of the oxidation parameter from wet chemical analyses of the two spherical samples D and E *a posteriori* were abandoned because of uncertainties involved in the actual analyses.

2.2 Investigation into the range of non-stoichiometry

2.2.1 *The relationship $\gamma' - \log p_{\text{O}_2}$.* The relationship between the apparent oxidation parameter γ' and the logarithm of oxygen partial pressure determined experimentally for TM60 at 1275 °C is represented by the solid line in Fig. 7. The course of the line is typical for an ionic compound which contains one volatile component (e.g. oxygen) and whose composition can vary to a certain extent depending on the chemical activity of the volatile component in the environment. A theoretical treatment of the relationship between a variable y which describes the departure from an ideal stoichiometric formula of an ionic compound (e.g. an oxide $\text{MO}_{1 \pm y}$) and its equilibrium oxygen partial pressure is given by, e.g. Greenwood (1970). A derivation of the $\gamma(p_{\text{O}_2})$ dependence based on a simple statistical treatment leads to the equation:

$$\sqrt{[p(y)/p(0)]} = [y + \sqrt{(y^2 + 4\delta^2)}]/2\delta \quad (4)$$

where y stands for the oxidation parameter, $p(y)$ and $p(0)$ are the partial pressures of oxygen in equilibrium with the non-stoichiometric ($\text{MO}_{1 \pm y}$), and the stoichiometric, (MO), oxide; δ is the so-called parameter of intrinsic disorder which tells what relative change in partial pressure of oxygen is needed to produce a given departure from stoichiometry y . In case of surplus oxygen, $y > 0$, vacancies are formed in the cationic sublattice of the oxide and $y = n_v/N$; here n_v is the number of cationic vacancies per unit volume and N is the total number of cation lattice sites per unit volume. One of the simplifications involved in derivation of the formula (4) is that the only type of defects are the cationic randomly distributed and non-interacting vacancies. Despite this and other simplifying assumptions, experiments show that equation (4) is in good agreement with the behaviour of non-stoichiometric compounds in a close vicinity of stoichiometric composition.

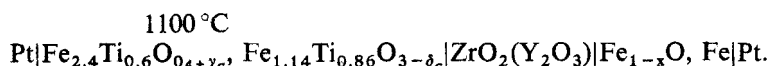
We have modified the formula (4) to suit our case of a ternary (basically ionic) oxide $\text{M}_3\text{O}_{4+\gamma}$. Solving it for y and replacing y by γ we obtained $\gamma = \delta' [p(y) - p(0)] / \sqrt{[p(y)p(0)]}$. A further simplification involved is that the formation of vacancies in the A and B lattice sites is taken as equally probable. The quantity δ' which can be obtained as an empirical constant from experiments is then roughly related to the parameter of intrinsic disorder: $\delta = \frac{3}{16}\delta'$. Substituting the co-ordinates of two experimental points A ($\gamma = 0.000$, $\log p_{\text{O}_2} = -9.2$) and B ($\gamma = 0.030$, $\log p_{\text{O}_2} = -6.82$) in the equation (4) we have obtained: $\delta' = 3.6 \times 10^{-4}$. The theoretical curve (dot-dash line in Fig. 7) was then computed.

2.2.2 *Verification of the TM60–HI86 invariant equilibrium at 1100 °C and determination of the critical oxidation parameter γ_c .* The composition of the haemo-ilmenite $\text{Fe}_{1.14}\text{Ti}_{0.86}\text{O}_3$ (HI86) which is conjugate to TM60 at 1100 °C was obtained by interpolation from data by Buddington & Lindsley (1964) who studied the titanomagnetite–haemoilmenite equilibria between 600 and 1100 °C in hydrothermal conditions, controlling the oxygen fugacities by solid buffers. The equilibrium oxygen

fugacity f_{O_2} for the above assemblage obtained also by interpolation equals $10^{-9.1}$ atm.

In order to verify the above data in 'dry' conditions we have applied the method of emf measurements with solid state electrolytic cells. This method has proved extremely useful for studying similar thermochemical problems involving iron-titanium oxides (Taylor & Schmalzried 1964; Taylor, Williams & McCallister 1972).

We have synthesized both conjugate partners by the sintering process described previously. The substances were then pulverized to about 3- μm particle size and mixed together in a 1:1 weight ratio. About 250 mg of this mixture were filled into the compartment of the solid state cell represented schematically:



The cell compartment containing the measured assemblage TM60-HI86 was formed by an impervious (yttria stabilized) zirconia crucible tightly closed by a lid from the same material to minimize the oxygen transfer via the gaseous phase. The cell was then heated up stepwise in a surrounding atmosphere of purified argon (with oxygen content of the order of 10^{-12} atm) until it reached 1100°C . The intermediate values of the emf were measured at 700, 800 and 900 $^\circ\text{C}$ at which points the temperature was held constant for 2 hr. At 1100°C (i.e. at the assumed invariant point A) the system was held for 6 hr. The emf readings expressed in terms of $-\log_{10} p_{\text{O}_2}$ and

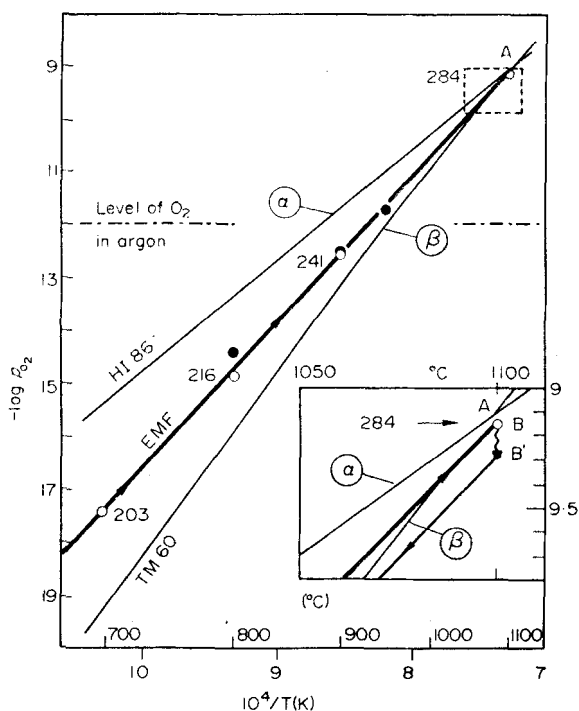


FIG. 5. The determination of oxygen partial pressure at 1100°C for the system $\text{Fe}_{2.4}\text{Ti}_{0.6}\text{O}_4\text{-Fe}_{1.14}\text{Ti}_{0.86}\text{O}_3$ by the method of emf measurements with solid state cells. The bold line marked EMF passing through the open circles (transient quasi-equilibria) and ending in the invariant point B (cf. the inset) shows the temperature variations of emf, converted to the $\log p_{\text{O}_2}$ values, as the cell was heated up. Measurements recorded on the cooling run are shown as solid circles. The thin lines labelled β and α , intersecting in point A are derived from measurements by Buddington & Lindsley. They represent the $\log p_{\text{O}_2}$ -temperature dependence for TM60 in equilibrium with the phase α and HI86 in equilibrium with the phase β . The figures attached to the points are emf readings in millivolts.

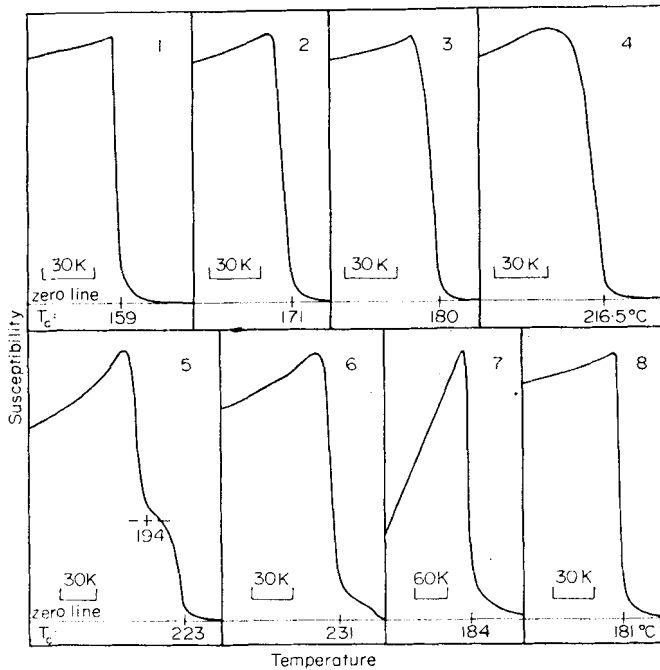


FIG. 6. Typical records of initial susceptibility (in arbitrary units) vs temperature for the samples of titanomagnetite TM60 in different state of oxidation or with different thermal history. The Curie temperature abscissae were determined as the projections of the drop onto the zero line. For convenience of drawing the records were reduced in size to the same peak height.

plotted against $1/T$ are shown in Fig. 5. The emf reading remained almost constant during the first 2 hr at the value of 284 mV ($10^{-9.14}$ atm) and then started to drift slightly. At the end of the 6-hr period the reading was 274 mV ($10^{-9.28}$ atm). This result is in very good agreement with the value $10^{-9.1}$ atm obtained by Buddington & Lindsley (1964) in the 'wet' system. The slight drift in our case may be caused by some loss of oxygen because of imperfect encapsulation of the measured assemblage which unlike a true binary mixture is not self-buffering. The intermediate emf readings on the heating up and cooling run do not, however, have much significance since the transient states through which the system was passing were not states of a true internal thermodynamic equilibrium. Complete equilibration at those points would have required a change in bulk composition and a re-distribution of Fe and Ti between the two phases.

Having confirmed the value of p_{O_2} for the 'dry' system we have determined the γ_c in the following way: three tablets weighing about 200 mg of the composition TM60, TM60+HI86 and HI86 were kept for 12 hr at 1100°C in a CO_2 -CO buffer ($p_{CO_2}/CO = 52/1$) giving the required oxygen partial pressure of $10^{-9.1}$ atm. The weight test and the X-ray test (with a Guinier deWolff camera) proved that the composition of all three tablets remained unchanged. There were no lines of α phase in the β phase and vice versa. The value of the critical oxidation parameter γ_c determined by chemical analysis of the TM60 tablet was: $\gamma_c(1100^\circ C) = 0.035 \pm 0.002$. The Curie point measurements on the samples cut out from the equilibrated tablets TM60 and TM60+HI86 yielded the values 181 and 184°C, respectively. (Cf. curves 8 and 7 in Fig. 6.) This renders a further proof that the composition of TM60 in the TM60-HI86 assemblage remained practically unaltered.

2.3 Curie point measurements

The Curie temperatures were measured by means of an apparatus devised by Stephenson & de Sa (1969). It is basically an ac susceptibility bridge driven by a 1.5 kHz oscillator, with the facility to vary the temperature of the sample *in situ* from 77 to 1000 K. The output from the bridge (directly proportional to the susceptibility) is displayed against temperature by means of an XY-recorder.

Several typical records of initial apparent susceptibility (in arbitrary units) *vs* temperature are shown in Fig. 6. As Curie temperatures we take the intercepts of the projected drop with the zero line. The sharpness of the transition makes it possible to determine the Curie point to about ± 1.5 K. The repeatability with the same sample is of the same order. The curves exhibit certain regularities in shape which correlate with the history of the sample:

(i) The virgin samples, i.e. those freshly prepared by double sintering and cooled slowly are much less stressed than the quenched ones and invariably exhibit the shape of curve No. 1. This curve is characterized by a moderate Hopkinson rise and by an extremely abrupt onset of the ferrimagnetic-paramagnetic transition with an almost vertical drop. If, however, a virgin sample is reheated and quenched, even without changing its state of oxidation, the typical sharp onset disappears and the shape of the curve No. 2 results.

(ii) An increasing degree of oxidation (as studied on the samples denoted D and E, fired at 1300 °C) leads to the typical sequence of curves shown as Nos 2, 3 and 4 for which the oxidation parameter varied $\gamma = 0.023, 0.033$ and 0.060 respectively. These three samples were quenched from 1275 °C.

(iii) Samples denoted A, B, C (firing temperature 1200 °C) were liable to behaviour represented by curve No. 6 which shows a flattening in its tail. This effect tends to grow stronger with increasing oxidation parameter. In a small number of cases it goes over into a distinct 'split' in the Curie temperature such as exhibited by curve No. 5. The 'split' resorbs when the sample is reduced to lower values of γ . This phenomenon may be indicative of a partial order-disorder transformation, but we have not attempted in this work to study it in any greater detail.

(iv) Curve No. 7 which shows a very strong Hopkinson effect was recorded with the synthetic sintered assemblage of TM60 + HI86. The sample of TM60 alone which was subjected to the same heat treatment (discussed above) yielded curve No. 8.

2.4 The dependence of the Curie temperature on the apparent oxidation parameter and the estimate of the true value of oxidation parameter.

The measured $T_c(\gamma')$ dependence is represented in Fig. 4 by the full straight line 1 which is drawn to obtain the best visual fit with the experimental points. In the upper part of the plot a break is observed near $\gamma' = 0.050$ which obviously corresponds to the boundary of the monophasic field β beyond which further oxidation produces the phase α . The steeper gradient may be associated with the gradual increase of the Fe/Ti ratio in the parent phase β as the titanium richer phase α exsolves. The $T_c(\gamma')$ dependence in the single phase region of TM60 is described by the equation

$$T_c(\gamma') = 161 + 890\gamma$$

(where T_c is given in °C).

In order to find at least an approximate 'true' value of the oxidation parameter γ we had recourse to an indirect way. This way is visualized in Fig. 4. The straight line 1 which represents the measured $T_c(\gamma')$ dependence is translated to the position 2 (without changing its gradient) as to fit the mean value of two experimental points A ($T_c = 150$ °C, $\gamma = 0.000 \pm 0.002$) and C ($T_c = 181$ °C, $\gamma = 0.035 \pm 0.002$) for which the

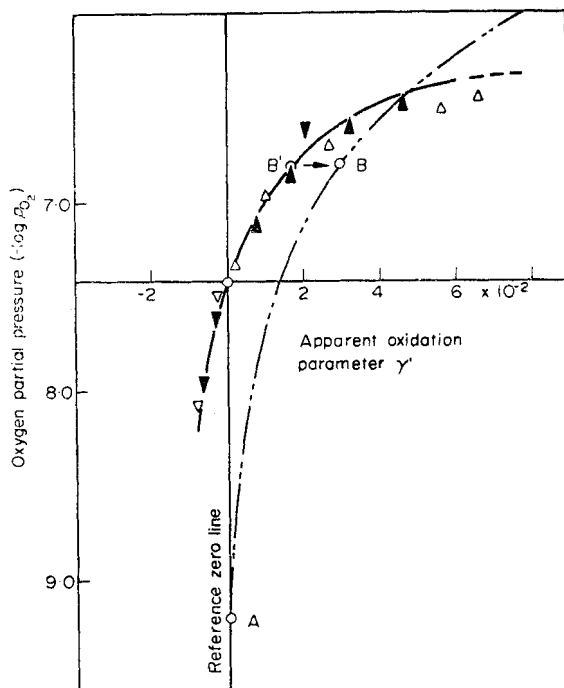


FIG. 7. The apparent oxidation parameter plotted as a function of oxygen partial pressure. The position of the triangles have the same meaning as in Fig. 4. The dash-dot line represents the $\gamma(\log p_{O_2})$ function calculated from a simple statistical model.

true value of the oxidation parameter was determined by wet chemical analyses. The translation operation yielded the transformation formula: $\gamma = \gamma' + 0.013$. The $T_c(\gamma)$ dependence obtained by the transformation is then

$$T_c(\gamma) = 149 + 890\gamma \text{ (}^\circ\text{C)}.$$

The co-ordinates for the point A were determined in the following way: A tablet of TM60 E weighing about 200 mg was equilibrated at 1275 °C in an atmosphere of $p_{O_2} = 10^{-9.2}$ atm; ($p_{CO_2} = 2.3 : 1$). Part of the tablet was then shaped into a sphere for the T_c measurements and the rest used for the determination of the Fe^{2+} content by wet chemical analyses. The weight percentages of Fe^{2+} obtained in a set of 5 analyses (titrations with ceric sulphate) were: 39.5; 39.4; 39.3; 39.3; 39.4. This gives an average of 39.4 ± 0.1 weight per cent of Fe^{2+} . The total amount of iron in the sample as well as the Fe : Ti ratio (4 : 1) were adjusted by careful synthesis and were subsequently confirmed by the electron probe microanalysis. Substituting the found percentage of divalent iron, 39.4 in the formula:

$$\gamma(\text{TM60}) = [0.4(2 - Fe^{2+}/(Fe_{\text{tot}} - Fe^{2+}))]/[1 + Fe^{2+}/(Fe_{\text{tot}} - Fe^{2+})]$$

we obtain $\gamma = 0.000 \pm 0.002$. The exact stoichiometric composition of the sample (within the analytical accuracy), although based on a calculated extrapolation of the equilibrium variables p_{O_2} and T came out rather fortuitously.

The co-ordinates for the point C were obtained from experiments carried out at 1100 °C in connection with the application of the method of electromotive force measurements as described previously.

3. Discussion

3.1 The difference in $T_c(\gamma)$ curves for TM60 oxidized in the lt and ht region are shown in Fig. 8. Curve 1 represents our experimental results. Curves 2 and 3 representing the lt experiments were obtained by interpolation or extrapolation from measurements carried out by Readman & O'Reilly (1972) and Ozima & Sakamoto (1972) respectively. Curves 4a and b are computed from Stephenson's formula (2). They stand for two extreme cases of initial cation distribution, *viz.* 4a applies to random (Akimoto) distribution while 4b applies to ordered (Néel-Chevalier) case.

There is a striking, almost an order-of-magnitude difference between the mean initial gradients \bar{k} ($\bar{k} = \delta T_c / \delta \gamma$) of the experimental curves 1 and 2 for which $\bar{k}_1 / \bar{k}_2 = 1/0.11$. Unfortunately, the measurements by Ozima & Sakamoto are not sufficiently detailed within the region of ($0 \leq \gamma \leq 0.1$) as to make any significant comparison. The curve 3 in the latter region is, in fact, a projection of a straight line fitted to experimental points which fall into an interval approximately $0.1 \leq \gamma \leq 0.2$. The intercept of curve 3 with abscissa $\gamma = 0$ gives $T_c \approx 20^\circ\text{C}$ for TM70, *i.e.* about 90°C for TM60 which is far too low. It is therefore necessary to assume that the curve 3 departs strongly from linearity in the region near the stoichiometric composition.

From the various comparisons it appears that the differences in the response of Curie temperature to oxidation of titanomagnetite TM60 at low and high temperature are far greater than can be explained as a scatter due to unavoidable differences involved in experiments of the above authors.

In discussing the possible nature of the differences between the two cases the molecular field theory extended by Stephenson to oxidized titanomagnetites provides a useful basis. It can be seen from the formula (2) that there are two kinds of phenomena

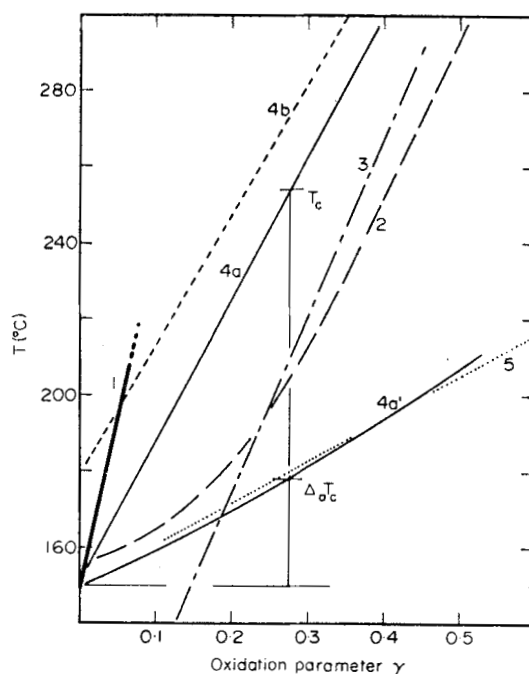


FIG. 8. Curie temperature of the titanomagnetite TM60 as a function of the oxidation parameter γ . A comparison of experimental (ex) and theoretical (th) results of different authors: Curve: 1(ex)—present work; 2(ex)—Readman & O'Reilly; 3(ex)—Ozima & Sakamoto; 4a, a' and b (th)—Stephenson; 5—calculated from Schult's experimental work.

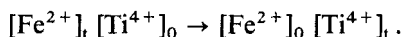
which have major effect upon the temperature of magnetic transition, T_c : (i) the cation distribution and (ii) interionic distances. As both are sensitive to the thermal history of a given specimen they are likely to be the cause of the discussed differences.

3.1.1 *Effect of cation distribution.* The oxidation of TM60 with initially disordered and ordered distribution of Fe^{3+} and Fe^{2+} into A and B lattice sites leads to the $T_c(\gamma)$ relationship represented by the 4a and 4b curves in Fig. 8. The calculated Curie points for stoichiometric disordered and ordered TM60 differ by 28 °C; the average initial gradients are $\bar{k}_{4a} = 375$ and $\bar{k}_{4b} = 350 \text{ K}\gamma^{-1}$. In accordance with the model of temperature dependent cation distribution in titanomagnetites as postulated by Stephenson (1969) any intermediate distribution should yield a $T_c(\gamma)$ curve contained between the two extreme cases (4a and b), and hence the relative change of gradient \bar{k} of oxidized samples quenched from high temperature and those which were oxidized slowly below 400 °C should not theoretically exceed 7 per cent.

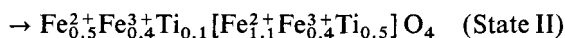
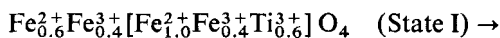
The distribution of ferric and ferrous ions between the octahedral and tetrahedral at equilibrium lattice sites in Stephenson's theory is governed by the Boltzman relation: $m_B n_A = m_A n_B \exp(-\Delta E/kT)$. The change in energy term ΔE connected with the interchange $(\text{Fe}^{3+})_A \rightarrow B$, $(\text{Fe}^{2+})_B \rightarrow A$ is in the above derivations assumed to be constant with respect to both composition (x) and temperature. It has been realized by Stephenson and later shown by Bleil (1971) that in a more refined treatment the latter assumption, $\Delta E = \text{const}$, ought to be replaced by $\Delta E \equiv \Delta E(x, T)$. It is probable that for oxidized titanomagnetites ΔE will also be affected by the parameter γ because formation of vacancies is bound to change the nearest neighbour configuration of cations and consequently the binding energies.

However, unless any drastic change of $\Delta E(\gamma)$ occurs within the interval of γ in question, ($0 < \gamma \lesssim 0.06$), the cation distribution alone cannot account for the observed difference.

In our previous consideration we have ignored the possibility of the Ti^{4+} ions being partly located in the tetrahedral sites. At the temperature of 1275 °C, however, one may assume that a number of Ti^{4+} would migrate from octahedral to tetrahedral sites, and that an appreciable fraction of that number would survive in tetrahedral sites on quenching. It is worth examining also this possibility. For the sake of simplicity let us consider the more probable interchange involving divalent iron only



To obtain an estimate, at least, as to the direction of change in T_c with respect to the above process it will suffice to compute T_c by the formula (2) for a particular degree of interchange in the titanomagnetite TM60. For instance, for initially disordered (Akimoto) distribution let us assume the following interchange



Transition from State I to II produces theoretically a change in Curie temperature 150 \rightarrow 149.5 °C respectively. In a similar way for initially ordered (Néel-Chevalier) distribution in TM60 the pertinent change of T_c is 178 \rightarrow 190 °C. It is, however, paradoxical to consider an initially ordered distribution in highly quenched TM60 and therefore only the former case may be considered. Thus the Curie temperature appears to be almost unaffected even if 17 per cent of the total number of Ti^{4+} in TM60 had migrated to tetrahedral sites.

3.1.2 *Effect of lattice parameter a on T_c .* The curve 4a and b computed from equation (2) might equally apply to both lt and ht cases as the underlying theory does not involve any *a priori* restrictions as to the temperature range at which a given titanomagnetite acquired an excess of oxygen. A certain bias for the lt case is however contained within the term $[8.4/a(\gamma)]^{13}$. In the numerical solution of equation (2), Stephenson for the sake of simplicity assumes that the lattice parameter is a linear function of the oxidation parameter; $a_\gamma = a_0(1 + \alpha\gamma)$, and that $\alpha = -0.0152$ for the whole titanomagnetite series. The value of α is inferred from the difference between lattice parameters of magnetite and maghemite, i.e. from a typically lt case.

Readman & O'Reilly (1972) have found experimentally that in the lt case the cell edge of titanomagnetites does not vary linearly with oxidation parameter. The $a(\gamma)$ dependence interpolated for TM60 from the experimental data of these authors is shown in Fig. 9 as curve 2. If, however, T_c is plotted against a , a straight line is obtained which for the above composition gives the following relation

$$T_c = 155\{1 + [8.48 - a(\gamma)] 2.2 \times 10^3\}.$$

The theoretical curve 4a' is drawn in Fig. 8 to illustrate how much the reduction of the lattice parameter brought about by oxidation contributes to the net change of T_c represented by the curve 4a. Denoting by $\Delta_a T_c$ the part which is dependent on the lattice parameter the relation describing the curve 4a' becomes:

$$\Delta_a T_c = [(8.4/a(\gamma))^{13} - (8.4/8.48)^{13}] 700\sqrt{(D - \Delta/D)}.$$

We can see that the average relative change $\Delta_a T_c / (T_c - 150) \approx 0.3$. It is interesting to note that the curve 4a' is corroborated by measurements of variations of Curie temperature with hydrostatic pressure (Schult 1970).

From direct measurements on TM60 Schult obtained for $\delta T_c / \delta p$ a value of $1.225^\circ\text{C}/1$ kbar which was practically constant over a range $0 < p < 50$ kbar.

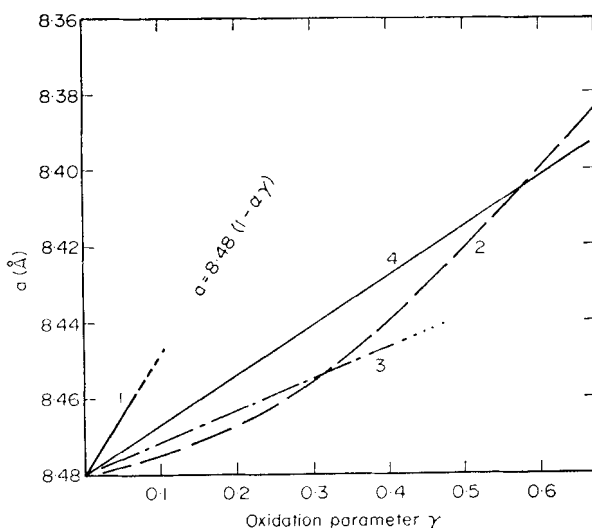


FIG. 9. Cell edge of the titanomagnetite TM60 as a function of the oxidation parameter γ . A comparison of experimental (ex) and theoretical (th) results of different authors: Curve 1, hypothetical, showing what cell edge contraction would be necessary to obtain a fit with the $T_c(\gamma)$ dependence calculated from Stephenson formula (2); Curve 2, (ex)—Readman & O'Reilly; Curve 3, (ex)—Ozima & Sakamoto; Curve 4, (th)—Stephenson.

Expressing the reduction in lattice parameter due to elastic compression in terms of equivalent of the γ parameter we arrive at a value for the gradient of $\delta(\Delta_a T_c)/\delta\gamma \approx 101 \text{ K}\gamma^{-1}$ (shown by the dotted line 5 in Fig. 8). This is in a very good agreement with the average slope $106 \text{ K}\gamma^{-1}$ of the curve 4a'.

3.1.3 Effect of quenching. Changes in interionic distances which may arise from oxidation and/or different heat treatment encompass processes in the crystal lattice of considerable complexity. We can discuss them only in a crude qualitative way.

Slow oxidation of titanomagnetites below the temperature of the irreversible spinel-corundum lattice transformation, i.e. $\sim 350^\circ\text{C}$ has been thoroughly studied and is fairly well understood. The spinel lattice in this region is capable of accommodating large concentrations of cationic vacancies which may order themselves giving rise to a superstructure. The arrival of 4 supernumerary oxygen atoms injects three vacancies into the cationic sublattice. At the temperature of about 250°C and, say $\gamma = 0.03$, the number of vacancies produced by oxidation, $n_{\text{ox}} \approx 2.5 \times 10^{19}$ per cm^3 , is much larger than the number of thermodynamically inherent, stoichiometrically balanced defects of Schottky and/or Frenkel type n_{in} which is 10^8 – 10^{10} per cm^3 . The concentration of the inherent Schottky defects is proportional to $\exp(-W_s/RT)$ where W_s is defined as the maximum work of formation of one 'gram-ion' of electrostatically balanced vacancies (in both cationic and anionic sublattices).

In the ht case, e.g. at 1275°C we have estimated that $n_{\text{in}} \approx 2 \times 10^{19}$. This means that at the same degree of oxidation as in the previous case, $\gamma = 0.03$, the number of balanced vacancies is of the same order as the γ -bound vacancies, n_{ox} . It is therefore possible that an efficient quenching can lead to a greater shrinkage of the lattice as a large number of inherent defects do not succeed in recombining and remain trapped in the lattice. Moreover, unlike the lt case at $\gamma = 0.03$, the TM60 lattice at 1275°C is highly saturated with the oxidation bound vacancies in the sense of the relative concentration, which can be defined as the ratio $\nu = n_{\text{ox}}/n_{\text{ox},c}$ where the denominator means a critical concentration corresponding to γ_c , i.e. the maximum number of vacancies which the phase β can tolerate. For the condition specified above $\nu \approx 0.5$ ($\gamma_c \approx 0.06$), whereas for the lt case and identical degree of oxidation $\nu \approx 0.04$.

The crystal lattice of TM60 with such a high value of $\nu = 0.5$ can no longer be regarded as a system of randomly distributed non-interacting monovacancies and interaction energies of processes such as clustering have to be taken into account. The concentration at which the simple statistical model of non-reacting vacancies ceases to be valid can be estimated from the graph in Fig. 7. The theoretical curve (dash dot) representing the $\gamma(\log p_{\text{O}_2})$ dependence which is based on the above simple model fits the experimental curve (solid) closely up to about $\gamma = 0.03$ whereupon it starts departing quite markedly. This may be understood in terms of rapidly increasing tendency of the vacancies to interact among themselves after a certain value of ν has been reached. For the studied case of TM60 this value of ν appears to be just about 0.5.

There are a variety of ways in which the vacancies can interact ranging from formation of relatively simple imperfections such as dislocation loops, by precipitation of vacancies, to formation of intricate patterns known as shear-structures or twin-structures which are accompanied by reduction in lattice symmetry. Moreover, the quenching of the specimens adds further imperfections and structural instabilities. It has been found by Lowrie & Fuller (1969) that imperfections introduced into the magnetite lattice by quenching lead, inter alia, to the strengthening of magnetic exchange interactions manifested, e.g. in increased Curie point and induced magnetization.

At the present stage of this study we cannot attribute the observed strong $T_c(\gamma)$ effect to any particular type of lattice imperfections neither can we decide whether it is the direct or indirect interaction which is the more strongly influenced.

For the time being it may suffice to consider the net effect of all the possible lattice imperfections as if the interionic distances were uniformly reduced throughout the crystal. Adopting the Stephenson equation (2) we can rectify it as to fit the observed values for the ht case. This will require the substitution of a hypothetical lattice shrinkage coefficient $\alpha' = 0.038 \gamma^{-1}$ instead of $\alpha = -0.0152 \gamma^{-1}$ which has been used to compute the curve 4a.

Generally, we conclude that the explanation to the observed strong $T_c(\gamma)$ dependence in quenched titanomagnetites is to be sought in the role of special imperfections rather than in the $\text{Fe}^{3+} - \text{Fe}^{2+}$ distribution of the Boltzmann type.

3.1.4 *The scatter in Curie point data of synthetic titanomagnetites.* The high sensitivity of the Curie temperature to the oxidation parameter in the ht case offers an explanation for the large scatter in existing experimental T_c data for pure synthetic titanomagnetites. Table 2 surveys some of the available figures for TM60 obtained by different authors.

Table 2

Reference	Curie point (°C)
T _c measured directly on pure TM60	
Bleil (1972)	210
Frölich (1970)	190
Lewis (1968)	220
Richards <i>et al.</i> (1973)	206
Schult (1970)	170
Present work	149
Interpolated values for TM60 from the T _c (x) curves	
Akimoto (1962)	156
Readman & O'Reilly (1972)	155
Robins (1972)	159

In view of the large scatter which is obvious from Table 2 it appears that for reliable measurements of Curie temperature an accurate determination of oxygen stoichiometry is of primary concern. So far, wet chemical analysis, chiefly the determination of Fe^{2+} , is the only way of obtaining the true value of the parameter γ . However, chemical analysis alone does not prove the phase uniformity and a check may be needed to ascertain that the studied sample does not contain any traces of the exsolved phase α . In particular, samples with relatively high T_c which were sintered at rather lower temperatures (850–1000 °C) should be suspect of containing exsolved phase α . On the other hand for homogeneous titanomagnetites the knowledge of $T_c(\gamma)$ dependence enables a reasonable estimate of the degree of deviation from stoichiometry, and, of the monophasic region's boundaries. This is, for example, useful for following the advancement of approaching stoichiometric composition of titanomagnetites in gaseous buffers, especially as a complementary information to weight changes. The advantage of such combination is that both measurements are relatively quick and non-destructive.

4. Conclusions

In the present investigation a combination of some methods of experimental petrology and magnetic measurements have been combined in attempting to elucidate certain problems relevant to palaeomagnetism. The main result is the very strong

dependence of Curie point on the high temperature non-stoichiometry found in titanomagnetite quenched from 1275 °C. Apart from intrinsic interest the present study may help in understanding thermomagnetic behaviour of such samples of igneous rock in which the occurrence of highly oxidized supercooled grains of titanomagnetites can be expected, such as geologically recent rapidly cooled submarine basalt or in thin lava flows. According to the present results titanomagnetites in such rocks should exhibit elevated Curie temperatures, up to about 50 K higher than the unoxidized ones. Equilibration of the metastable supercooled grains at moderate temperatures (~ 500 °C) is likely to be accompanied by significant changes of Curie temperature.

Acknowledgments

This work forms a part of a research programme in rock and mineral magnetism 'Thermoremanence in titanomagnetites' sponsored by the Natural Environment Research Council of the UK under the general supervision of Professor K. M. Creer whose guidance and encouragement is gratefully acknowledged. The author wishes also to thank Dr W. O'Reilly for stimulating discussions and for his help with preparing the manuscript, and Dr B. C. H. Steele from the Royal School of Mines, Imperial College, London for help with the emf measurements with solid state cells.

*Department of Geophysics and Planetary Physics,
School of Physics,
The University of Newcastle upon Tyne, NE1 7RU.*

References

- Akimoto, S., 1962. Magnetic properties of FeO-Fe₂O₃-TiO₂ system as a basis of rock magnetism, *J. Phys. Soc. Japan.*, **17**, Suppl. B-1, 706-710.
- Bleil, U., 1971. Cation distribution in titanomagnetites, *Z. für Geophysik*, **37**, 305-319.
- Bleil, U., 1972. Quoted by Stephenson, A., 1972b.
- Buddington, A. F. & Lindsley, D. H., 1964. Iron-titanium oxide minerals and synthetic equivalents, *J. Petrology*, **5**, 310-357.
- Creer, K. M. & Ibbetson, J. D., 1970. Electron microprobe analyses and magnetic properties of non-stoichiometric titanomagnetite in basaltic rocks, *Geophys. J. R. astr. Soc.*, **21**, 485-511.
- Fröhlich, F., 1970. Beiträge zum Erkundungsprogramm: Materieparameter im Bereich der Erdkruste, Veröffentlichungen des Zentralinstituts Physik der Erde, Nr. 4, Deutsche Akademie der Wissenschaften zu Berlin.
- Greenwood, N. N., 1970. *Ionic crystals lattice defects and nonstoichiometry*, Butterworth, London.
- Lewis, M., 1968. Some experiments on synthetic titanomagnetites, *Geophys. J. R. astr. Soc.*, **16**, 295-310.
- Lowrie, W. & Fuller, M., 1969. Effect of annealing on coercive force and remanent magnetization in magnetite, *J. geophys. Res.*, **74**, 2698-2710.
- Ozima, M. & Sakamoto, N., 1972. Magnetic properties of synthesized titanomagnetites, *J. geophys. Res.*, **76**, 7035-7046.
- Readman, P. W. & O'Reilly, W., 1970. The synthesis and inversion of nonstoichiometric titanomagnetites, *Phys. Earth Planet. Int.*, **4**, 121-128.
- Readman, P. W. & O'Reilly, W., 1971. Oxidation processes in titanomagnetites, *Z. geophys.*, **37**, 329-338.
- Readman, P. W. & O'Reilly, W., 1972. Magnetic properties of oxidized (cation-deficient) titanomagnetites (Fe,Ti, □)₃O₄, *J. geomag. geoelectr.* **24**, 69-90.

- Richards, J. C. W., O'Donovan, J. B., Hauptman, Z., O'Reilly, W. & Creer, K. M., 1973. A magnetic study of titanomagnetite substituted by magnesium and aluminium, *Phys. Earth Planet. Int.*, **7**, 437–444.
- Robins, B. W., 1972. *Remanent magnetization in spinel iron-oxides*, Ph.D. Thesis, University of New South Wales.
- Schult, A., 1970. Effect of pressure on the Curie temperature of titanomagnetites $(1-x)\text{Fe}_3\text{O}_4-x\text{TiFe}_2\text{O}_4$, *Earth Planet. Sci. Lett.*, **10**, 81–86.
- Stephenson, A., 1969. The temperature dependent cation distribution in titanomagnetites, *Geophys. J. R. astr. Soc.*, **18**, 199–210.
- Stephenson, A. & de Sa, A., 1969. A simple method for the measurement of the temperature variation of initial magnetic susceptibility between 77 and 1000 K, *J. Phys. E.*, **3**, 59–61.
- Stephenson, A., 1972a. Spontaneous magnetization curves and Curie points of spinels containing two types of magnetic ion, *Phil. Mag.*, **25**, 1213–1232.
- Stephenson, A., 1972b. Spontaneous magnetization Curves and Curie points of cation deficient titanomagnetites, *Geophys. J. R. astr. Soc.*, **29**, 91–107.
- Taylor, R. W., 1963. Liquidus temperatures in the system $\text{FeO}-\text{Fe}_2\text{O}_3-\text{TiO}_2$, *J. Am. Ceram. Soc.*, **46**, 276–279.
- Taylor, R. W., 1964. Phase equilibria in the system $\text{FeO}-\text{Fe}_2\text{O}_3-\text{TiO}_2$ at 1300 °C, *Am. Min.*, **49**, 1016–1030.
- Taylor, R. W. & Schmalzried, H., 1964. The free energy of formation of some titanates silicates and magnesium aluminate from measurements made with galvanic cells involving solid electrolytes, *J. Phys. Chem.*, **68**, 2444–2449.
- Taylor, L. A., Williams, R. J. & McCallister, R. H., 1972. Stability relations of ilmenite and ulvöspinel in the Fe-Ti-O system and application of these data to lunar mineral assemblages, *Earth Planet. Sci. Letters*, **16**, 282–288.